





Disk transport rates from Ti isotopic signatures of refractory inclusions

Jan RENDER ^{1,4*}, James F. J. BRYSON ², Samuel EBERT ³, and Gregory A. BRENNECKA ¹

¹Lawrence Livermore National Laboratory, 7000 East Avenue, Livermore, California 94550, USA

²Department of Earth Sciences, University of Oxford, South Parks Road, Oxford OX1 3AN, UK

³Institut für Planetologie, University of Münster, Wilhelm-Klemm-Str. 10, 48149 Münster, Germany

⁴Westfälische Wilhelms-Universität Münster, Wilhelm-Klemm-Str. 10, 48149 Münster, Germany

*Corresponding author. E-mail: render1@llnl.gov

(Received 03 February 2022; revision accepted 17 October 2022)

Abstract—The early solar system was a dynamic period during which the formation of early solids set into motion the process of planet building. Although both astrophysical observations and theoretical modeling demonstrate the presence of widespread transport of material, we lack concrete quantitative constraints on timings, distances, and mechanisms thereof. To trace these transport processes, one needs objects of known early formation times and these objects would need to be distributed throughout parent bodies with known accretion times and distances. Generally, these criteria are met by “regular” (i.e., non-fractionated and unidentified nuclear and excluding hibonite-rich) Ca-Al-rich inclusions (CAIs) as these objects formed very early and close to the young Sun and contain distinctive nucleosynthetic isotope anomalies that permit provenance tracing. However, nucleosynthetic isotopic signatures of such refractory inclusions have so far primarily been analyzed in chondritic meteorites that formed within ~4 AU from the Sun. Here, we investigate Ti isotopic signatures of four refractory inclusions from the ungrouped carbonaceous chondrite WIS 91600 that was previously suggested to have formed beyond ~10 AU from the Sun. We show that these inclusions exhibit correlated excesses in ⁵⁰Ti and ⁴⁶Ti and lack large Ti isotopic anomalies that would otherwise be indicative of more enigmatic refractory materials with unknown formation ages. Instead, these isotope systematics suggest the inclusions to be genetically related to regular CAIs commonly found in other chondrites that have a broadly known formation region and age. Collectively, this implies that a common population of CAIs was distributed over the inner ~10 AU within ~3.5 Myr, yielding an average (minimum) speed for the transport of millimeter-scale material in the early solar system of ~1 cm s⁻¹.

INTRODUCTION

Among the events that occurred in the early solar system are myriad processes and reactions that led to solid formation and planet building. One of the most consequential of these processes for the eventual compositions and locations of planetary bodies was the widespread transport of matter throughout the protoplanetary disk. Whereas many models have been proposed to explain the movement and eventual current arrangement of material in the solar system (e.g.,

Chambers & Wetherill, 1998; Ciesla, 2007; Desch et al., 2018; Lambrechts & Johansen, 2012), quantitative time-scales, distances, and underlying mechanisms of the transport of various objects recovered from laboratory measurements of materials that date from the very early solar system are lacking.

The first solids that formed within the solar system are widely thought to have been assemblages of refractory minerals, referred to as Ca-Al-rich inclusions, or CAIs. Due to their atypical mineralogical compositions, these objects must have formed in a high-temperature environment that is often assumed to have existed close (<1 AU) to the young Sun (Bekaert et al. [2021] and references therein) and prior to bulk meteorite and

[Correction added on 27 Jan 2023, after first online publication: Second affiliation to Jan Render was added.]

planetesimal accretion (Connelly et al., 2017; MacPherson et al., 2012). In this period, the Sun was in a more active pre-main sequence phase that provided the necessary physicochemical conditions for CAI formation for <200,000 years (Cieza et al., 2007). Although having formed in a broadly similar environment, however, these refractory inclusions are found in a wide range of materials—from a variety of chondritic meteorites, interplanetary dust particles, and even cometary material (Joswiak et al., 2017; Matzel et al., 2010; McKeegan et al., 1998). As such, not only are refractory inclusions evidence for substantial material transport throughout the disk, but they are also highly diagnostic tracer materials for mixing and transport early in solar system history. Perhaps most notably, comet Wild 2 contains such refractory materials (e.g., Joswiak et al., 2017; Matzel et al., 2010), highlighting that materials from the inner solar system were transported distally to the cometary formation regions in the outer solar system. And, while the observation of refractory minerals in Wild 2 qualitatively argues for significant outward transport of inner solar system material, such evidence remains qualitative due to uncertainties on the radial accretion distance of Wild 2.

Because refractory materials come in different types, it is important to understand the different materials' relationships to each other to have an accurate accounting of solar system materials. Specifically, these inclusions range from ultrarefractory hibonite-rich grains found in CM and CR chondrites (e.g., platy hibonite crystals [PLACs] and/or spinel–hibonite inclusions [SHIBs]; e.g., Kööp, Davis, et al., 2016; Kööp, Nakashima, et al., 2016), to the more enigmatic (F)UN (fractionated and unidentified nuclear) inclusions (e.g., Kööp et al., 2018; Krot et al., 2014) and “regular” (i.e., non-FUN and excluding hibonite-rich) inclusions, which are commonly found in various chondrite groups. The latter type, “regular” CAIs, exhibit relatively small ranges in nucleosynthetic isotope anomalies compared to (F)UN inclusions and hibonite-rich grains, which exhibit anomalies up to the percent level (Dauphas & Schauble, 2016; Shollenberger et al., 2022). This observation is compatible with “regular” CAIs having formed in an isotopically more homogeneous formation region, and perhaps in a comparatively limited spatial and temporal framework. This idea is additionally supported by both long- and short-lived isotope chronometers, that attest “regular” CAIs (from here on just referred to as simply “CAIs”) to have formed within ~40,000 to 200,000 years (e.g., Connelly et al., 2017; Kawasaki et al., 2019; MacPherson et al., 2012), consistent with the abovementioned pre-main sequence stage of the young Sun (Brennecka et al., 2020). Critically, this abbreviated formation period is not only observed for larger sized inclusions from CV chondrites (Jacobsen et al., 2008) but

also for regular CAIs from ordinary, CO, CR, and CM chondrites (Makide et al., 2009; Matzel et al., 2013; Russell et al., 1996; Ushikubo et al., 2017), all of which exhibit (near-)canonical initial ^{26}Al abundances (i.e., $^{26}\text{Al}/^{27}\text{Al}_0 \approx 5 \times 10^{-5}$). And whereas the spatial and temporal formation conditions of FUN CAIs and hibonite-rich inclusions are less well constrained, isotopic anomalies of nucleosynthetic origin remain a powerful tool for discriminating between these different types of refractory inclusions.

One particularly useful element for determining the genetic kinship of refractory inclusions is titanium (Ti). Because Ti is a highly refractory element, it is present as a major constituent of refractory inclusions, allowing the Ti isotopic composition to be measured with high fidelity, even in inclusions with sub-millimeter diameters (Ebert et al., 2018; Render et al., 2019). Furthermore, Ti has five stable isotopes (^{46}Ti , ^{47}Ti , ^{48}Ti , ^{49}Ti , and ^{50}Ti) that are formed in a variety of nucleosynthetic environments, meaning that Ti isotopic signatures can provide information about the stellar sources that contributed matter to the solar system (e.g., Steele et al., 2012). Additionally, since the Ti isotope signatures of materials such as PLACs, SHIBs, (F)UN inclusions, and CAIs are well documented (Dauphas & Schauble, 2016; Davis et al., 2018; Render et al., 2019), the genetic relationship of the different types of inclusions is well established based on their related $^{46}\text{Ti}/^{47}\text{Ti}$ and $^{50}\text{Ti}/^{47}\text{Ti}$ signatures (Davis et al., 2018; Render et al., 2019). Here, we leverage Ti isotopic signatures of CAIs located in a carbonaceous chondrite that has been proposed to have assembled far more distally than the parent bodies of most other meteorites to shed quantitative light on the timings and distances of the transport and mixing of millimeter-scale solids in the early protoplanetary disk.

SAMPLES

WIS 91600

Wisconsin Range (WIS) 91600 was first classified as a C2 carbonaceous chondrite with an affinity toward the CM group (Choe et al., 2010). WIS 91600 is similar to Belgica 7904 and Y-86720, which all exhibit bulk chemical compositions similar to CM chondrites; however, these three meteorites have undergone more extensive aqueous alteration than CM chondrites. All three chondrites exhibit unusual oxygen isotopic compositions ($\Delta^{17}\text{O} \approx 0$, close to CI carbonaceous chondrites) and appear to have been moderately heated, inducing several changes to these meteorites, most notably the partial dehydration of phyllosilicates compared to traditional CMs (e.g., Lentfort et al., 2021;

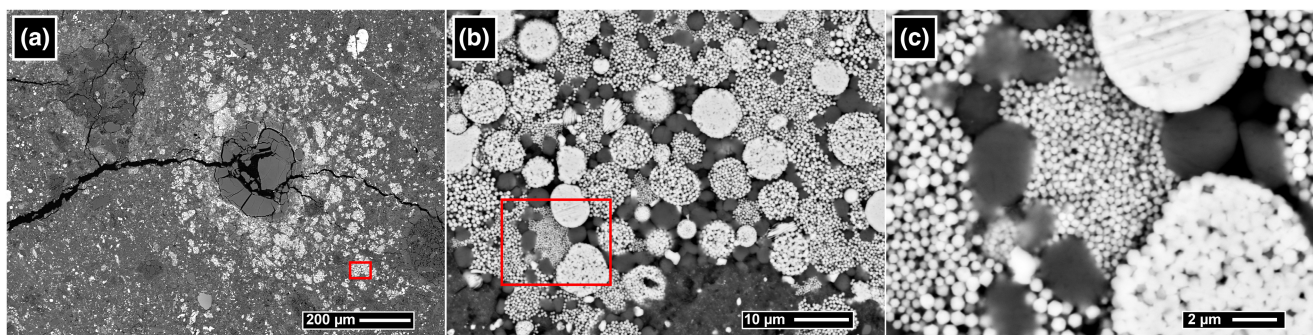


Fig. 1. a–c) Backscattered electron (BSE) images of an area in WIS 91600 showing framboidal magnetite spheres, indicating a petrologic type 2.0 or lower for the aliquot used in this study.

Rubin et al., 2007). As such, these three chondrites have been proposed to represent either a grouplet of anomalous CM chondrites or even potentially a new distinct group of chondrites known as the CY chondrites (King et al., 2019). Whereas WIS 91600 has been broadly classified as petrologic type 2.4 (Choe et al., 2010), the presence of magnetite (Fig. 1) and the lack of tochilinite–cronstedtite intergrowths (TCIs) indicate a petrologic type 2.0 or lower for the specific piece used in our study. This range of petrologic characteristics being found in samples of the same meteorite suggests that the parent body had variable environmental conditions. Regardless of the exact characteristics of any specific piece, the broad extensive aqueous alteration and CM/CY-like properties suggest that members of this proposed grouplet/group had a distal formation region, particularly compared to the parent bodies of ordinary and enstatite chondrites that exhibit far lower degrees of aqueous alteration. To this end, recent work by Bryson, Weiss, Biersteker, et al. (2020) used the magnetic remanence carried by WIS 91600 and proposed that the parent body(ies) of these meteorites formed more distally than those of most other meteorites (including extensively aqueously altered chondrites like CM chondrites), placing a nominal quantitative constraint on this distance of ≥ 9.8 AU (details in Material S3 in supporting information).

CAI Samples

Two thick sections of WIS 91600 were examined for CAIs using the JEOL 6610 secondary electron microscope (SEM) at the University of Münster. Due to the extensive and ubiquitous aqueous alteration (e.g., Fig. 1), many primary phases had been destroyed or transformed; however, a handful of refractory inclusions were identified by the presence of spinel and perovskite as well as their overall shape and appearance. Out of the inclusions of interest, only four CAIs were identified that were large enough for isotopic investigation. These samples range

from ~ 0.05 to ~ 0.15 mm² (Fig. 2a–d), at the upper end of sizes reported for CM CAIs (Ebert et al., 2019; MacPherson, 2014; Rubin, 2011). Bulk chemical compositions of these four CAIs were characterized using energy-dispersive X-ray spectroscopy (EDS) and these data are presented in Table S1 in supporting information.

The four WIS CAIs show evidence of having been subjected to severe aqueous alteration, resulting in the mineral assembly often being dominated by alteration products (Fig. 2). Therefore, it was not possible to infer the original mineralogical composition or perform unambiguous classification of the subtypes of these inclusions. The shape of CAI-1 suggests it is a fragment, yet a circular character is visible, indicating that this inclusion may have been a compact type CAI at one time. Its interior has been reworked to secondary alteration phases, whereas spinel along with small perovskite grains are present in the rim. CAI-2 is irregularly shaped, with spinel present on only one side of the inclusion. Similar to CAI-1, it is possible that this object is a fragment of a previously disrupted inclusion. CAI-3 is an elongated and irregularly shaped inclusion with spinel present as small grains throughout the object, suggesting it was formerly a porous spinel–pyroxene-rich aggregate or a distended chain of spinel nodules—common in CM chondrites (MacPherson, 2014). Lastly, CAI-4 is also irregularly shaped, but the boundary between the CAI and the matrix is more recognizable for this CAI than CAI-3. Spinel is the main phase with small grains of perovskite also present, along with secondary phases. As a result of the extensive alteration, none of the four inclusions show evidence of Ca-pyroxene, a common phase found in many other CM CAIs.

METHODS

Sample Removal

After characterization, the CAIs were removed from the WIS 91600 section following the method of Charlier

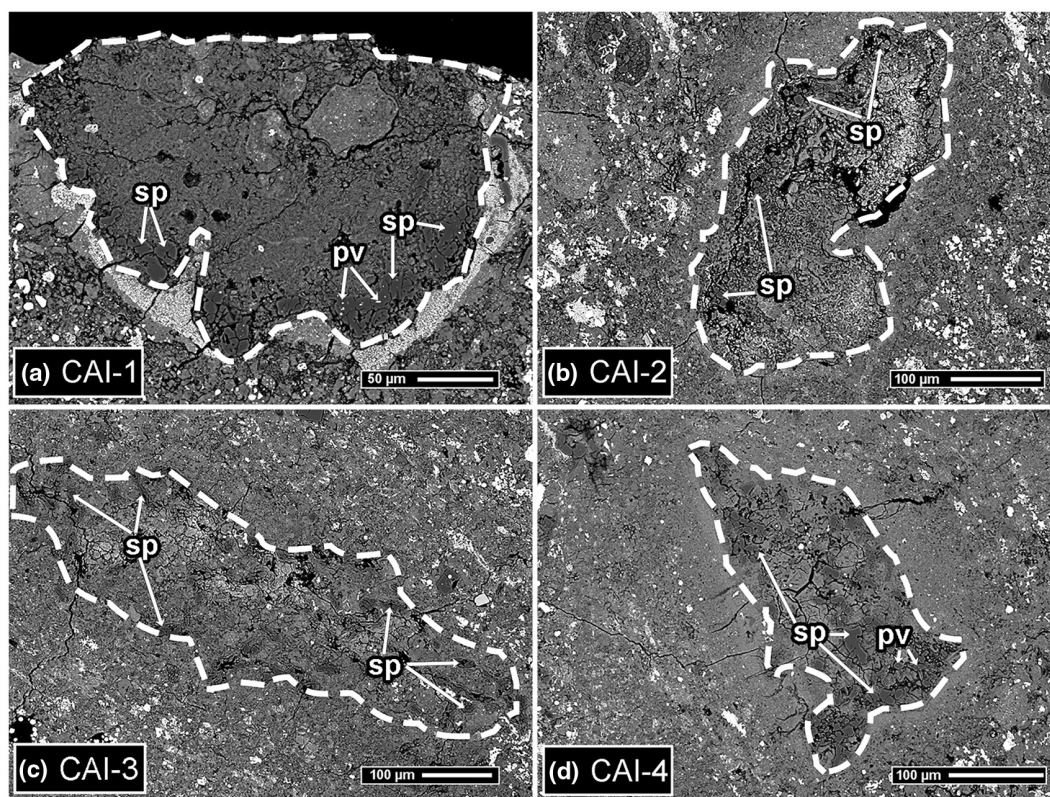


Fig. 2. a–d) Backscattered electron (BSE) images of the investigated CAI samples. White dashed lines mark the area of the investigated CAI. sp = spinel; pv = perovskite.

et al. (2006), as outlined in our previous study (Render et al., 2019). In brief, thick sections of the meteorite were mounted in a New Wave Research Micro Mill, and a droplet of Milli-Q water was placed on the meteorite surface. By drilling through the water droplet into the area of interest, a suspension was created that was transferred into PFA beakers using a pipette. Even though the inclusions described here were the largest ones present in our aliquot of WIS 91600, these CAIs were smaller than the minimum drill hole dimensions, making it inevitable that some surrounding host chondrite material was included with the sample during removal, as shown in Fig. 3.

Dissolution of the drilled out material was performed using table-top digestion in concentrated HNO_3 -HF and reverse aqua regia for several days each on a hotplate at 180 °C. After digestion, the samples were dried down and re-dissolved in 12 M HNO_3 for Ti purification following the method of Torrano et al. (2019). Procedural blanks of this chemical purification procedure are ~ 2 ng Ti and yields are $\geq 70\%$. This sample set was accompanied by BCR-2 and an aliquot (48.7 mg) of the bulk WIS 91600 chondrite.

Ti Isotope Measurements

Titanium isotope measurements were performed using the Neptune *Plus* MC-ICPMS in combination with a Cetac Aridus II[®] desolvator at the Institut für Planetologie in Münster and internally normalizing to $^{49}\text{Ti}/^{47}\text{Ti} = 0.749766$. Analyses were performed in medium resolution mode and on the left shoulder of the peak plateau to avoid a gaseous interference on mass 50 (Render et al., 2019). Results are given in ϵ -notation, as parts-per-ten-thousand deviations relative to the Origins Lab OL-Ti standard:

$$\epsilon^i\text{Ti} = \left[\frac{(^i\text{Ti}/^{47}\text{Ti})_{\text{sample}}}{(^i\text{Ti}/^{47}\text{Ti})_{\text{standard}}} - 1 \right] \times 10,000.$$

The analytical uncertainty of our method was determined from the twofold standard deviation of a total of 20 analyses of the terrestrial basalt standard BCR-2, yielding external reproducibilities for $\epsilon^{46}\text{Ti}$, $\epsilon^{48}\text{Ti}$, and $\epsilon^{50}\text{Ti}$ of 0.68, 0.66, and 0.78 for 50 ng g^{-1} Ti solutions and 0.50, 0.29, and 0.49 for 100 ng g^{-1} Ti solutions, respectively.

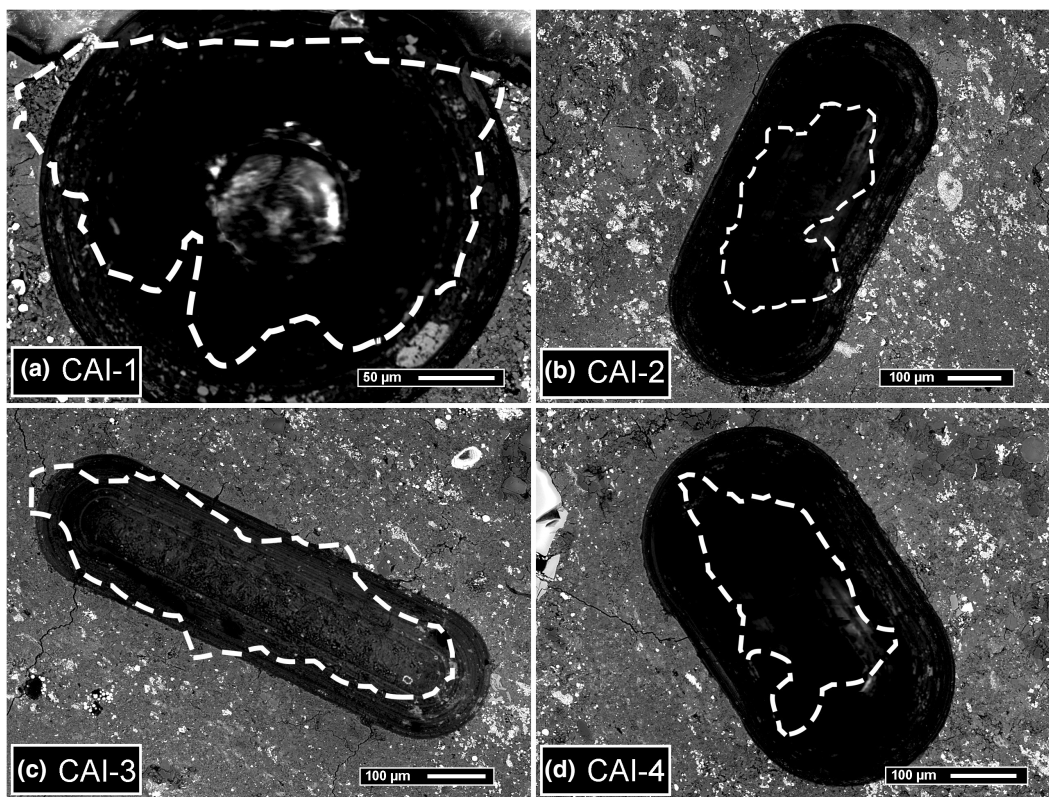


Fig. 3. a–d) Pictures of the samples investigated in this study after removal using the microdrill. Dashed lines indicate the approximate area of the CAI, also shown in Fig. 2.

As visible in Fig. 3, Ti from the surrounding host meteorite was included to various degrees during excavation of the four inclusions. Following Ebert et al. (2018) and Render et al. (2019), we therefore performed corrections on the measured Ti isotopic composition to subtract any potential effects from incidentally incorporated host chondrite material. To this end, the fraction of CAI material in each drill hole was calculated by comparing the pre- and post-removal photographs, allowing for the contribution of the host meteorite to be subtracted from the measured value to calculate the original Ti isotopic composition of the CAI (details given in Material S2 in supporting information and in Render et al., 2019). In the following sections, the given Ti isotopic compositions of CAIs always refer to the corrected values. We emphasize that even the highest correction of 0.36 ϵ -units (applied to the $\epsilon^{50}\text{Ti}$ isotopic composition of “CAI 1”) is smaller than the analytical uncertainty achieved here, indicating that the incidental inclusion of surrounding host meteorite material during the drilling process only has a minor effect on the Ti isotopic compositions reported.

RESULTS AND DISCUSSION

Ti Isotope Signatures

Ti isotopic compositions of standards and samples and their associated uncertainties are shown in Table 1 and Fig. 4. To verify the accuracy of our method, we analyzed our internal laboratory CAI standard, the sample “Egg-2 high” as well as the terrestrial basalt standard USGS BCR-2 in the same analytical session. Both standards yielded Ti isotopic compositions that are typical for a CV CAI (Egg-2 high) as well as of a terrestrial sample (BCR-2) and that are indistinguishable from previously reported Ti isotopic signatures for these particular samples (e.g., Ebert et al., 2018; Gerber et al., 2017; Render et al., 2019; Zhang et al., 2011).

Our bulk aliquot of WIS 91600 exhibits positive Ti isotopic anomalies in $\epsilon^{46}\text{Ti}$ and $\epsilon^{50}\text{Ti}$, whereas its ^{48}Ti value is not resolved from BCR-2 (Table 1), all of which are in good agreement with previously published Ti isotopic compositions of CM chondrites and the ungrouped chondrite Tagish Lake (Trinquier et al., 2009), demonstrating the close genetic kinship

Table 1. Mass-independent Ti isotopic compositions of terrestrial and CAI samples investigated in this study.

Sample	TiO ₂ (wt%) ^a	<i>f</i> _{CAI}	ppb Ti _{sol}	<i>N</i> ^b	ε ⁴⁶ Ti ^c	ε ⁴⁸ Ti ^c	ε ⁵⁰ Ti ^c
Egg-2 high			100	1	1.82 ± 0.50	0.71 ± 0.29	9.85 ± 0.49
BCR-2			50	10	-0.23 ± 0.21	0.07 ± 0.21	0.16 ± 0.25
			100	10	-0.24 ± 0.16	-0.09 ± 0.09	-0.16 ± 0.16
WIS 91600 bulk	0.057		300	5	0.63 ± 0.10	-0.05 ± 0.03	2.81 ± 0.15
CAI 1 ^d	0.17	0.70	50	2	-0.03 ± 0.68	—	-0.06 ± 0.80
CAI 2	0.36	0.30	100	3	0.94 ± 0.50	0.63 ± 0.30	3.17 ± 0.49
CAI 3 ^d	0.10	0.82	50	2	0.56 ± 0.68	—	1.18 ± 0.79
CAI 4	0.54	0.28	100	3	0.99 ± 0.50	0.28 ± 0.29	4.36 ± 0.52

^aTiO₂ concentration in weight percent as determined by SEM-EDS for CAIs and by quadrupole ICPMS for bulk WIS 91600. *f*_{CAI} denotes the fraction of CAI material per sample.

^bNumber of analyses of the same sample solution.

^cNucleosynthetic Ti isotope data are reported using the ε-notation relative to the OL-Ti reference standard and are mass-bias corrected by internally normalizing to ⁴⁹Ti/⁴⁷Ti = 0.749766 and using the exponential law. For samples measured >3 times, uncertainties are twofold standard errors (2 SE) from replicate analyses; for samples measured ≤3 times, uncertainties reflect the external reproducibility as defined by 2 × standard deviation (2 SD) of repeated analyses of BCR-2. Measured Ti isotopic compositions of the WIS CAIs were corrected for incidental inclusion of host chondrite material (Fig. 3) and final uncertainties include a 50% propagation from these corrections (details given in Material S2).

^dNo ε⁴⁸Ti isotope data reported due to low Ti contents and more significant interferences from ⁴⁸Ca during these measurements.

between these carbonaceous chondrites. However, whereas both Tagish Lake and CM chondrites typically exhibit Ti concentrations of ~550 μg g⁻¹ (e.g., Braukmüller et al., 2018), we determined a comparatively lower Ti abundance of 339 μg g⁻¹ for our aliquot of WIS 91600 (corresponding to 0.057 wt% TiO₂, Table 1), which is more akin to the Ti concentration reported for CI chondrites (~400 μg g⁻¹ Ti; Braukmüller et al., 2018). Consistent with this observation, the section of WIS 91600 investigated here also exhibits a more CI-like structure and modal mineralogy: typical CM phases, such as TCIs, are completely absent, whereas framboidal magnetite is omnipresent (Fig. 1). Similar observations have been previously made for other anomalous CM and C2 chondrites such as Essebi, Bells, and Tagish Lake (e.g., Brearley, 1995; Brown et al., 2000; Patzek et al., 2018). In these chondrites, the framboidal magnetite typically results from heavy and progressive alteration under the presence of aqueous fluids and the breakdown of tochilinite (McSween, 1987; Tomeoka & Buseck, 1985).

Similarly, all four refractory inclusions investigated here underwent extensive aqueous alteration as indicated by the abundance of alteration products and magnetite surrounding CAI-1 (Fig. 2). The reason for the presence of this magnetite-rich rim surrounding only one of the four CAIs is currently not known but may indicate that CAI-1 may have had a rim that differed in mineralogy to that of the other CAIs. Furthermore, evidence from other CAIs found in a thin section of WIS 91600 (not measured here) shows multiple highly altered spinel and Al-rich regions where the Al-phases have been largely destroyed and paired with low-Ti

content CAIs, suggesting that CAIs in this meteorite have been, in general, significantly altered.

A survey of 20 refractory inclusions from the Mighei CM chondrite yielded an average ~2 wt% TiO₂ (MacPherson & Davis, 1994), whereas samples of this study contained systematically less TiO₂, ranging between 0.10 and 0.56 wt% (note, however, that the abovementioned survey also included hibonite-bearing inclusions, which is a Ti-bearing mineral that is absent in the inclusions investigated here). The WIS CAIs also contain lower Ti concentrations compared to “regular” CAIs from other chondrite groups that—while variable from sample to sample—typically contain 0.5–2 wt% TiO₂ (e.g., Ebert et al., 2018; Render et al., 2019; Stracke et al., 2012). This dearth of Ti could be indigenous to these WIS CAIs or, alternatively, the lack of Ti could in principle be a function of the significant aqueous and metamorphic alteration observed in this aliquot of WIS 91600.

Similarly, the four CAIs in this study exhibit relatively small isotopic anomalies in the most diagnostic isotope (ε⁵⁰Ti) ranging from ~0 (CAI 1) to ~4.5 (CAI 4) ε-units compared to other CAIs that often display excesses of ~9 ε. In fact, there appears to be a link (*R*² = 0.83) between Ti concentration and ε⁵⁰Ti in the four CAIs investigated in this study. However, given that Ti is not typically considered a mobile element under most conditions (e.g., Gaillardet et al., 2014), it appears rather unlikely that most of the initial Ti in these CAIs has been redistributed. Instead, we currently presume that the abovementioned link between Ti concentration and Ti isotopic composition is coincidental and may result from the relatively small number of inclusions

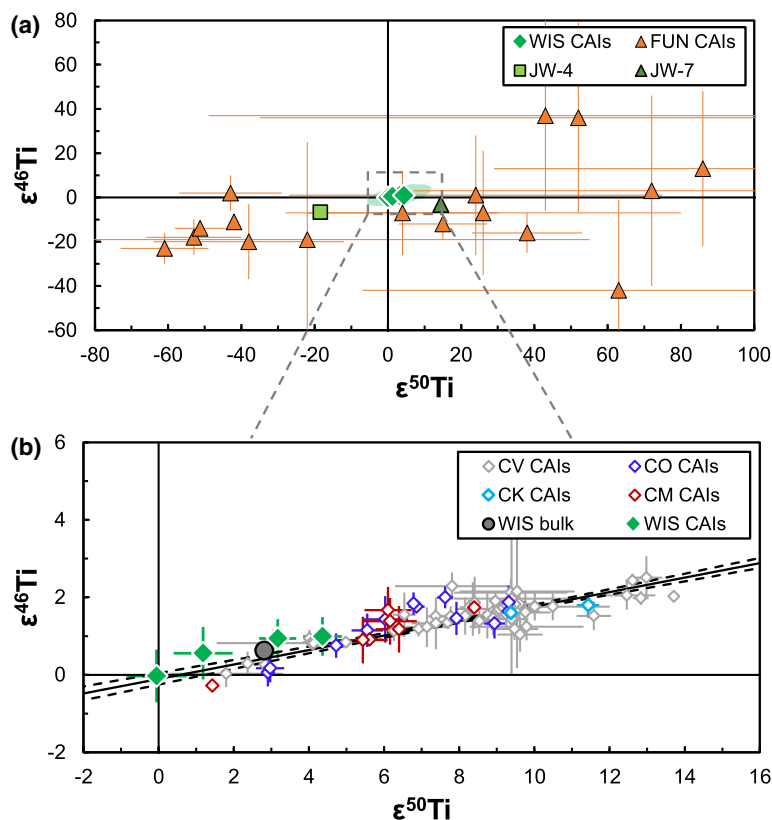


Fig. 4. a) Nucleosynthetic Ti isotopic compositions of the four inclusions from WIS 91600 reported here are distinct from Ti isotope data of hibonite-rich and FUN CAIs (Kööp et al., 2018; Loss et al., 1994; Niederer et al., 1980, 1981; Park et al., 2014; Williams et al., 2016) and the two hibonite-rich inclusions from the CM chondrite Jbilet Winselwan (Render et al., 2019) (note that hibonite-rich grains can be far more isotopically anomalous [Kööp, Davis, et al., 2016; Kööp, Nakashima, et al., 2016]). b) Instead, all four WIS 91600 inclusions studied here fall along the linear regression previously defined for “regular” CAIs (Shollenberger et al. [2022] and references therein). Uncertainties of JW-4, JW-7, and bulk WIS 91600 are smaller than the symbols.

studied here. Consistent with this hypothesis, the bulk WIS 91600 Ti isotope signature is also indistinguishable to previously reported nucleosynthetic Ti isotope anomalies of CM chondrites that WIS 91600 has been suggested to be related to. This is despite the severe aqueous alteration of our section of bulk WIS 91600 and its comparatively low Ti concentration, indicating that mass-independent Ti isotopic compositions are not substantially affected during secondary alteration and the potential redistribution of Ti.

Lastly, we note that even if these CAIs lost some of their Ti during aqueous alteration of WIS 91600, the inclusions investigated here are still enriched in Ti compared to the surrounding material. Specifically, and despite their dearth in Ti, the CAIs still contain ~3 to ~10 times more Ti than their host meteorite (Table 1). Importantly, any potential mixing of host rock Ti with CAI Ti would only shift the measured CAI signal slightly closer to the bulk rock instead of drastically altering the isotopic character of a CAI. Thus, it is

possible that the Ti isotope anomalies of the inclusions have been diluted to smaller magnitudes; however, it would be very difficult to overprint the isotopic character of the inclusions (Ebert et al., 2018). Considering that both FUN CAIs and hibonite-rich inclusions are vastly different in their Ti isotopic compositions (Fig. 4), it would require >100 times the original Ti content of the inclusions to effectively overprint such highly anomalous Ti isotopic signatures.

Potential Genetic Relationships to Different CAI Families

The primary goal of this study is to determine if the inclusions located in WIS 91600—even if potentially modified by aqueous alteration—are genetically related to well-studied CAIs found in other carbonaceous chondrites. As mentioned above, the four inclusions investigated here are distinguishable in their Ti isotopic compositions, but even when CAIs from various host meteorites have different absolute nucleosynthetic

anomalies, their relationship to one another can be probed using isotope anomaly ratios.

For regular CAIs, this genetic kinship is recognizable in correlated $\epsilon^{46}\text{Ti}$ versus $\epsilon^{50}\text{Ti}$ anomalies (Davis et al., 2018; Render et al., 2019), with almost all inclusions analyzed so far plotting along a well-defined array ($\epsilon^{46}\text{Ti} = [0.188 \pm 0.015] \times \epsilon^{50}\text{Ti} - [0.10 \pm 0.14]$; Shollenberger et al., 2022). In contrast, earlier formed solids, such as PLACs and SHIBs, not only display considerably larger isotopic anomalies but also lack this correlation in Ti isotope anomalies (e.g., Kööp, Davis, et al., 2016; Kööp, Nakashima, et al., 2016). As evident from their vastly different isotopic characters, these hibonite-rich inclusions as well as (F)UN CAIs do not share the same isotopic heritage and must have captured different mixtures of isotopically anomalous matter compared to regular CAIs. Combining the $\epsilon^{46}\text{Ti}$ and $\epsilon^{50}\text{Ti}$ of a sample thus provides a means to test the genetic relationship of individual refractory inclusions.

Three of the four WIS 91600 inclusions measured here exhibit distinguishable excesses in $\epsilon^{50}\text{Ti}$, and two display positive anomalies in $\epsilon^{46}\text{Ti}$. Even though these anomalies are more muted compared to many other CAIs from other meteorites, all four inclusions measured in this study fall along the previously defined $\epsilon^{46}\text{Ti}$ - $\epsilon^{50}\text{Ti}$ correlation line (Fig. 4), strongly suggesting that these WIS 91600 CAIs incorporated similar mixtures of presolar matter and thus likely share a common origin with CAIs from other chondrites. It is yet unclear why CAIs have variable isotopic anomalies in certain elements (e.g., Ti, Ni, Sr, Mo, W; Brennecka et al., 2020; Render et al., 2018); however, proposed explanations include that one source of material during the CAI-forming epoch was isotopically anomalous, and/or that late-infalling material from the solar system's parental molecular cloud had variable isotopic signatures due to changes in the isotopic composition of this infall (Brennecka et al., 2020; Jacquet et al., 2019; Nanne et al., 2019). As such, inclusions spanning the $\epsilon^{46}\text{Ti}$ - $\epsilon^{50}\text{Ti}$ correlation could possibly represent CAIs that formed at slightly different times during the infall and/or incorporated moderately more or less of similarly sourced isotopically anomalous Ti phases. As formation ages for these four inclusions in particular have not been reported, their precise chronology is unknown; however, based on extensive prior chronology (Connelly et al., 2017; Kawasaki et al., 2019; MacPherson et al., 2012), the population of CAIs is generally thought to have been formed within $\leq 200,000$ years during the Sun's pre-main sequence phase (Brennecka et al., 2020).

Considering the vast differences in mineralogical composition and isotopic character between CAIs and other early solids, these four refractory inclusions from WIS 91600 appear unrelated to (F)UN CAIs and

hibonite-rich inclusions and display characteristics that are typical for regular CAIs. Collectively, these observations indicate that the four inclusions analyzed here formed broadly contemporaneously together with CAIs from other carbonaceous chondrites and within ≤ 1 AU of the Sun.

Implications for Solar System Transport Processes

Based on the measured magnetic remanence carried by WIS 91600 (Bryson, Weiss, Biersteker, et al., 2020) compared to that carried by individual chondrules extracted from several meteorites (Borlina et al., 2021; Fu et al., 2014, 2020), bulk meteorites (Bryson, Weiss, Lima, et al., 2020; Cournede et al., 2015), and magnetohydrodynamical models of the protoplanetary disk (Bai, 2015; Bai & Goodman, 2009; Weiss et al., 2021), the parent body of WIS 91600 has been argued to originate notably more distally than those of most of meteorite groups, potentially at >10 AU (a detailed discussion of these comparisons is presented in Material S3 in supporting information).

As indicated by their Ti isotopic and mineralogical signatures, the four WIS CAIs studied here are most consistently related to CAIs found in the more well-studied carbonaceous chondrite groups (e.g., CM, CV, CR chondrites). This link is important because such regular CAIs are thought to have formed close to the Sun (<1 AU; Bekaert et al., 2021) in a geologically brief window of time ($<200,000$ years; Connelly et al., 2017; Kawasaki et al., 2019; MacPherson et al., 2012), and their presence in a meteorite that formed distally in the solar system at ~ 3.5 Myr (Sugiura & Fujiya, 2014) provides some of the first quantitative constraints on the time scales and distances of the transport of millimeter-scale material in the early solar system. This is consistent with the more recent notion that CAIs were already present in the CC region prior to achondrite (Render et al., 2022) and iron meteorite (Zhang et al., 2022) formation (i.e., <1 Myr after solar system formation). Taking the conservatively approximated values of 0.5 AU for CAI formation and 3.5 Myr after CAI formation for the accretion of the WIS 91600 parent body at 9.8 AU, we calculate a first-order approximation of the transport speed of millimeter-scale objects in the early protoplanetary disk of ~ 400 km year⁻¹. This first estimate fails to capture any of the caveats resulting from the uncertainties of the formation/accretion ages of CAIs and the WIS 91600 parent body, as well as of the distances of their formation. Addressing this shortcoming is possible by employing a Monte Carlo approach ($N = 30,000$ cycles), which provides a perhaps more reliable estimate of the average transport speed and assigns an uncertainty to this assessment (see Material S4

in supporting information). To this end, we integrate the abovementioned formation times and locations of CAIs and WIS 91600 to a transport distance of 9.3 ± 2.0 AU over a transfer period 3.5 ± 1.0 million years. Using these parameters, our model yields an average transport speed of 410 ± 170 km year⁻¹ or, on a more human scale, 1.2 ± 0.5 cm s⁻¹ (2 SD).

Of course, this calculated average transport speed is unable to capture the highly turbulent nature of disk dynamics, nor does it account for any potential travel above the midplane of the disk. As such, it represents a minimum rate based on a direct line distance from the source and the production and accretion ages of the materials involved. Similarly, the previously reported WIS 91600 accretion distance of ~ 9.8 AU represents a minimum distance for CAI transport—this could extend well into cometary accretion areas of >30 AU (e.g., Joswiak et al., 2017; Matzel et al., 2010). Nonetheless, this work demonstrates how to genetically connect material formed at a broadly known time and location in the inner solar system to its settling place in the outer solar system at a known time and location. As such, our investigation provides a fundamental constraint on the rates of transport of millimeter-scale material in the early solar system that could help to shed light on the dynamics of dust, gas, and solids within this structure.

Acknowledgments—This work was supported by a Sofja Kovalevskaja Award from the Alexander von Humboldt Foundation to G.A.B. as well as by the Laboratory Directed Research and Development program at LLNL under proposal number 20-ERD-001. This study was performed under the auspices of the U.S. Department of Energy by Lawrence Livermore National Laboratory under contract DE-AC52-07NA27344 with release number LLNL-JRNL-831252. This work was partly funded by the Deutsche Forschungsgemeinschaft, Germany (DFG, German Research Foundation)—project number 463342295. Z. Torrano is thanked for insightful discussions regarding FUN CAIs. The authors are furthermore grateful to A. Trinquier and A. Davis for constructive reviews that helped improve the manuscript, as well as Y. Marrocchi for efficient editorial handling. US Antarctic meteorite samples are recovered by the Antarctic Search for Meteorites (ANSMET) program, which has been funded by NSF and NASA and characterized and curated by the Department of Mineral Sciences of the Smithsonian Institution and Astromaterials Acquisition and Curation Office at NASA Johnson Space Center. Open Access funding enabled and organized by Projekt DEAL.

Conflict of Interest—The authors declare that they have no known competing financial interests or personal

relationships that could have appeared to influence the work reported in this paper.

Data Availability Statement—All data generated during this study are included in this article (and its supplementary information files).

Editorial Handling—Dr. Yves Marrocchi

REFERENCES

- Bai, X. N. 2015. Hall-Effect-Controlled Gas Dynamics in Protoplanetary Disks. II. Full 3D Simulations Toward the Outer Disk. *The Astrophysical Journal* 798: 84–101.
- Bai, X. N., and Goodman, J. 2009. Heat and Dust in Active Layers of Protostellar Disks. *The Astrophysical Journal* 701: 737–55.
- Bekaert, D. V., Auro, M., Shollenberger, Q. R., Liu, M.-C., Marschall, H., Burton, K. W., Jacobsen, B., et al. 2021. Fossil Records of Early Solar Irradiation and Cosmolocation of the CAI Factory: A Reappraisal. *Science Advances* 7: eabg8329.
- Borlina, C. S., Weiss, B. P., Bryson, J. F. J., Bai, X.-N., Lima, E. A., Chatterjee, N., and Mansbach, E. N. 2021. Paleomagnetic Evidence for a Disk Substructure in the Early Solar System. *Science Advances* 7: eabj6928.
- Braukmüller, N., Wombacher, F., Hezel, D. C., Escoube, R., and Münker, C. 2018. The Chemical Composition of Carbonaceous Chondrites: Implications for Volatile Element Depletion, Complementarity and Alteration. *Geochimica et Cosmochimica Acta* 239: 17–48.
- Brearley, A. J. 1995. Aqueous Alteration and Brecciation in Bells, an Unusual, Saponite-Bearing, CM Chondrite. *Geochimica et Cosmochimica Acta* 59: 2291–317.
- Brennecke, G. A., Burkhardt, C., Budde, G., Kruijjer, T. S., Nimmo, F., and Kleine, T. 2020. Astronomical Context of Solar System Formation from Molybdenum Isotopes in Meteorite Inclusions. *Science* 370: 837–40.
- Brown, P. G., Hildebrand, A. R., Zolensky, M. E., Grady, M., Clayton, R. N., Mayeda, T. K., Tagliaferri, E., et al. 2000. The Fall, Recovery, Orbit, and Composition of the Tagish Lake Meteorite: A New Type of Carbonaceous Chondrite. *Science* 290: 320–5.
- Bryson, J. F. J., Weiss, B. P., Biersteker, J. B., King, A. J., and Russel, S. S. 2020. Constraints on the Distances and Timescales of Solid Migration in the Early Solar System from Meteorite Magnetism. *The Astrophysical Journal* 896: 103–28.
- Bryson, J. F. J., Weiss, B. P., Lima, E. A., Gattacceca, J., and Cassata, W. S. 2020. Evidence for Asteroid Scattering and Distal Solar System Solids from Meteorite Paleomagnetism. *The Astrophysical Journal* 892: 126–49.
- Chambers, J. E., and Wetherill, G. W. 1998. Making the Terrestrial Planets: N-Body Integrations of Planetary Embryos in Three Dimensions. *Icarus* 136: 304–27.
- Charlier, B. L. A., Ginibre, C., Morgan, D., Nowell, G. M., Pearson, D. G., Davidson, J. P., and Ottley, C. J. 2006. Methods for the Microsampling and High-Precision Analysis of Strontium and Rubidium Isotopes at Single Crystal Scale for Petrological and Geochronological Applications. *Chemical Geology* 232: 114–33.

- Choe, W. H., Huber, H., Rubin, A. E., Kallemeyn, G. W., and Wasson, J. T. 2010. Compositions and Taxonomy of 15 Unusual Carbonaceous Chondrites. *Meteoritics & Planetary Science* 45: 531–54.
- Ciesla, F. J. 2007. Outward Transport of High-Temperature Materials Around the Mid-Plane of the Solar Nebula. *Science* 318: 613–5.
- Cieza, L., Padgett, D. L., Stapelfeldt, K. R., Augereau, J.-C., Harvey, P., Evans, N. J., II, Merin, B., et al. 2007. The Spitzer c2d Survey of Weak-Line T Tauri Stars. II. New Constraints on the Timescale for Planet Building. *The Astrophysical Journal* 667: 308–28.
- Connelly, J. N., Bollard, J., and Bizzarro, M. 2017. Pb-Pb Chronometry and the Early Solar System. *Geochimica et Cosmochimica Acta* 201: 345–63.
- Cournede, C., Gattacceca, J., Gounelle, M., Rochette, P., Weiss, B. P., and Zanda, B. 2015. An Early Solar System Magnetic Field Recorded in CM Chondrites. *Earth and Planetary Science Letters* 410: 62–74.
- Dauphas, N., and Schauble, E. A. 2016. Mass Fractionation Laws, Mass-Independent Effects, and Isotopic Anomalies. *Annual Review of Earth and Planetary Sciences* 44: 709–83.
- Davis, A. M., Zhang, J., Greber, N. D., Hu, J., Tissot, F. L. H., and Dauphas, N. 2018. Titanium Isotopes and Rare Earth Patterns in CAIs: Evidence for Thermal Processing and Gas-Dust Decoupling in the Protoplanetary Disk. *Geochimica et Cosmochimica Acta* 221: 275–95.
- Desch, S. J., Kalyaan, A., and Alexander, C. M. O'D. 2018. The Effect of Jupiter's Formation on the Distribution of Refractory Elements and Inclusions in Meteorites. *The Astrophysical Journal Supplement Series* 238: 11–41.
- Ebert, S., Bischoff, A., Harries, D., Lentfort, S., Barrat, J.-A., Pack, A., Gattacceca, J., Visser, R., Schmid-Beurmann, P., and Kimpel, S. 2019. Northwest Africa 11024—A Heated and Dehydrated Unique Carbonaceous (CM) Chondrite. *Meteoritics & Planetary Science* 54: 328–56.
- Ebert, S., Render, J., Brennecka, G. A., Burkhardt, C., Bischoff, A., Gerber, S., and Kleine, T. 2018. Ti Isotopic Evidence for a Non-CAI Refractory Component in the Inner Solar System. *Earth and Planetary Science Letters* 498: 257–65.
- Fu R. R., Kehayias P., Weiss B. P., Schrader D. L., Bai X.-N., and Simon J. B. 2020. Weak Magnetic Fields in the Outer Solar Nebula Recorded in CR Chondrites. *Journal of Geophysical Research* 125: e2019JE006260.
- Fu, R. R., Weiss, B. P., Lima, E. A., Harrison, R. J., Bai, X.-N., Desch, S. J., Ebel, D. S., et al. 2014. Solar Nebula Magnetic Fields Recorded in the Semarkona Meteorite. *Science* 346: 1089–92.
- Gaillardet, J., Viers, J., and Dupre, B. 2014. Trace Elements in River Waters. In *Treatise on Geochemistry*, edited by H. D. Holland and K. K. Turekian, 2nd ed., 195–235. Oxford: Elsevier.
- Gerber, S., Burkhardt, C., Budde, G., Metzler, K., and Kleine, T. 2017. Mixing and Transport of Dust in the Early Solar Nebula as Inferred from Titanium Isotope Variations Among Chondrules. *The Astrophysical Journal* 841: L17–23.
- Jacobsen, B., Yin, Q.-Z., Moynier, F., Amlin, Y., Krot, A. N., Nagashima, K., Hutcheon, I. D., and Palme, H. 2008. ^{26}Al - ^{26}Mg and ^{207}Pb - ^{206}Pb Systematics of Allende CAIs: Canonical Solar Initial $^{26}\text{Al}/^{27}\text{Al}$ Ratio Reinstated. *Earth and Planetary Science Letters* 272: 353–64.
- Jacquet, E., Pignatale, F. C., Chaussidon, M., and Charnoz, S. 2019. Fingerprints of the Protosolar Cloud Collapse in the Solar System. II. Nucleosynthetic Anomalies in Meteorites. *The Astrophysical Journal* 884: 32–42.
- Joswiak, D. J., Brownlee, D. E., Nguyen, A. N., and Messenger, S. 2017. Refractory Materials in Comet Samples. *Meteoritics & Planetary Science* 52: 1612–48.
- Kawasaki, N., Park, C., Sakamoto, N., Park, S. Y., Kim, H. N., Kuroda, M., and Yurimoto, H. 2019. Variations in Initial $^{26}\text{Al}/^{27}\text{Al}$ Ratios Among Fluffy Type A Ca-Al-Rich Inclusions from Reduced CV Chondrites. *Earth and Planetary Science Letters* 511: 25–35.
- King, A. J., Bates, H. C., Krietsch, D., Busemann, H., Clay, P. L., Schofield, P. F., and Russell, S. S. 2019. The Yamato-Type (CY) Carbonaceous Chondrite Group: Analogues for the Surface of Asteroid Ryugu? *Geochemistry* 79: 125531.
- Kööp, L., Davis, A. M., Nakashima, D., Park, C., Krot, A. N., Nagashima, K., Tenner, T. J., Heck, P. R., and Kita, N. T. 2016. A Link Between Oxygen, Calcium and Titanium Isotopes in ^{26}Al -Poor Hibonite-Rich CAIs from Murchison and Implications for the Heterogeneity of Dust Reservoirs in the Solar Nebula. *Geochimica et Cosmochimica Acta* 189: 70–95.
- Kööp, L., Nakashima, D., Heck, P. R., Kita, N. T., Tenner, T. J., Krot, A. N., Nagashima, K., Park, C., and Davis, A. M. 2016. New Constraints on the Relationship Between ^{26}Al and Oxygen, Calcium, and Titanium Isotopic Variation in the Early Solar System from a Multielement Isotopic Study of Spinel-Hibonite Inclusions. *Geochimica et Cosmochimica Acta* 184: 151–72.
- Kööp, L., Nakashima, D., Heck, P. R., Kita, N. T., Tenner, T. J., Krot, A. N., Nagashima, K., Park, C., and Davis, A. M. 2018. A Multielement Isotopic Study of Refractory FUN and F CAIs: Mass-Dependent and Mass-Independent Isotope Effects. *Geochimica et Cosmochimica Acta* 221: 296–317.
- Krot, A. N., Nagashima, K., Wasserburg, G. J., Huss, G. R., Papanastassiou, D., Davis, A. M., Hutcheon, I. D., and Bizzarro, M. 2014. Calcium-Aluminum-Rich Inclusions with Fractionation and Unknown Nuclear Effects (FUN CAIs): I. Mineralogy, Petrology, and Oxygen Isotopic Compositions. *Geochimica et Cosmochimica Acta* 145: 206–47.
- Lambrechts, M., and Johansen, A. 2012. Rapid Growth of Gas-Giant Cores by Pebble Accretion. *Astronomy and Astrophysics* 544: A32.
- Lentfort, S., Bischoff, A., Ebert, S., and Patzek, M. 2021. Classification of CM Chondrite Breccias—Implications for the Evaluation of Samples from the OSIRIS-REx and Hayabusa 2 Missions. *Meteoritics & Planetary Science* 56: 127–47.
- Loss, R. D., Lugmair, G. W., Davis, A. M., and MacPherson, G. J. 1994. Isotopically Distinct Reservoirs in the Solar Nebula: Isotope Anomalies in Vigarano Meteorite Inclusions. *The Astrophysical Journal* 436: L193–6.
- MacPherson, G. J. 2014. Calcium–Aluminum-Rich Inclusions in Chondritic Meteorites. In *Meteorites and Cosmochemical Processes, Treatise on Geochemistry*, edited by A. M. Davis, H. D. Holland, and K. K. Turekianvol. 1, 139–79. Oxford: Elsevier.
- MacPherson, G. J., and Davis, A. M. 1994. Refractory Inclusions in the Prototypical CM Chondrite, Mighei. *Geochimica et Cosmochimica Acta* 58: 5599–625.

- MacPherson, G. J., Kita, N. T., Ushikubo, T., Bullock, E. S., and Davis, A. M. 2012. Well-Resolved Variations in the Formation Ages for Ca–Al-Rich Inclusions in the Early Solar System. *Earth and Planetary Science Letters* 331–332: 43–54.
- Makide, K., Nagashima, K., Krot, A. N., Huss, G. R., Hutcheon, I. D., and Bischoff, A. 2009. Oxygen- and Magnesium-Isotope Compositions of Calcium–Aluminum-Rich Inclusions from CR2 Carbonaceous Chondrites. *Geochimica et Cosmochimica Acta* 73: 5018–50.
- Matzel, J. E. P., Ishii, H. A., Joswiak, D., Hutcheon, I. D., Bradley, J. P., Brownlee, D., Weber, P. K., et al. 2010. Constraints on the Formation Age of Cometary Material from the NASA Stardust Mission. *Science* 328: 483–6.
- Matzel, J. E. P., Simon, J. I., Hutcheon, I. D., Jacobsen, B., Simon, S. B., and Grossman, L. 2013. Oxygen Isotope Measurements of a Rare Murchison Type A CAI and its Rim (Abstract #2632). 44th Lunar and Planetary Science Conference. CD-ROM.
- McKeegan, K. D., Leshin, L. A., Russell, S. S., and MacPherson, G. J. 1998. Oxygen Isotopic Abundances in Calcium–Aluminum-Rich Inclusions from Ordinary Chondrites: Implications for Nebular Heterogeneity. *Science* 280: 414–7.
- McSween, H. Y., Jr. 1987. Aqueous Alteration in Carbonaceous Chondrites: Mass Balance Constraints on Matrix Mineralogy. *Geochimica et Cosmochimica Acta* 51: 2469–77.
- Nanne, J. A. M., Nimmo, F., Cuzzi, J. N., and Kleine, T. 2019. Origin of the Non-Carbonaceous–Carbonaceous Meteorite Dichotomy. *Earth and Planetary Science Letters* 511: 44–54.
- Niederer, F. R., Papanastassiou, D. A., and Wasserburg, G. J. 1980. Endemic Isotopic Anomalies in Titanium. *The Astrophysical Journal* 240: L73–7.
- Niederer, F. R., Papanastassiou, D. A., and Wasserburg, G. J. 1981. The Isotopic Composition of Titanium in the Allende and Leoville Meteorites. *Geochimica et Cosmochimica Acta* 45: 1017–31.
- Park, C., Nagashima, K., Wasserburg, G. J., Hutcheon, I. D., Davis, A. M., Huss, G. R., Bizzarro, M., and Krot, A. N. 2014. Calcium and Titanium Isotopic Compositions of FUN CAIs: Implications for their Origin (Abstract #2656). 45th Lunar and Planetary Science Conference. CD-ROM.
- Patzek, M., Bischoff, A., Visser, R., and John, T. 2018. Mineralogy of Volatile-Rich Clasts in Brecciated Meteorites. *Meteoritics & Planetary Science* 53: 2519–40.
- Render, J., Brennecka, G. A., Burkhardt, C., and Kleine, T. 2022. Solar System Evolution and Terrestrial Planet Accretion Determined by Zr Isotopic Signatures of Meteorites. *Earth and Planetary Science Letters* 595: 11748.
- Render, J., Brennecka, G. A., Wang, S.-J., Wasylenki, L. E., and Kleine, T. 2018. A Distinct Nucleosynthetic Heritage for Early Solar System Solids Recorded by Ni Isotope Signatures. *The Astrophysical Journal* 862: 26–43.
- Render, J., Ebert, S., Burkhardt, C., Kleine, T., and Brennecka, G. A. 2019. Titanium Isotopic Evidence for a Shared Genetic Heritage of Refractory Inclusions from Different Carbonaceous Chondrites. *Geochimica et Cosmochimica Acta* 254: 40–53.
- Rubin, A. E. 2011. Origin of the Differences in Refractory-Lithophile-Element Abundances Among Chondrite Groups. *Icarus* 213: 547–58.
- Rubin, A. E., Trigo-Rodríguez, J. M., Huber, H., and Wasson, J. T. 2007. Progressive Aqueous Alteration of CM Carbonaceous Chondrites. *Geochimica et Cosmochimica Acta* 71: 2361–82.
- Russell, S. S., Srinivasan, G., Huss, G. R., Wasserburg, G. J., and MacPherson, G. J. 1996. Evidence for Widespread ²⁶Al in the Solar Nebula and Constraints for Nebula Time Scales. *Science* 273: 757–62.
- Shollenberger, Q., Render, J., Jordan, M. K., McCain, K. A., Ebert, S., Bischoff, A., Kleine, T., and Young, E. D. 2022. Titanium Isotope Systematics of Refractory Inclusions: Echoes of Molecular Cloud Heterogeneity. *Geochimica et Cosmochimica Acta* 324: 44–65.
- Steele, R. C. J., Coath, C. D., Regelous, M., Russell, S., and Elliott, T. 2012. Neutron-Poor Nickel Isotope Anomalies in Meteorites. *The Astrophysical Journal* 758: 59.
- Stracke, A., Palme, H., Gellissen, M., Münker, C., Kleine, T., Birbaum, K., Günther, D., Bourdon, B., and Zipfel, J. 2012. Refractory Element Fractionation in the Allende Meteorite: Implications for Solar Nebula Condensation and the Chondritic Composition of Planetary Bodies. *Geochimica et Cosmochimica Acta* 85: 114–41.
- Sugiura, N., and Fujiya, W. 2014. Correlated Accretion Ages and $\epsilon^{54}\text{Cr}$ of Meteorite Parent Bodies and the Evolution of the Solar Nebula. *Meteoritics & Planetary Science* 49: 772–87.
- Tomeoka, K., and Buseck, P. R. 1985. Indicators of Aqueous Alteration in CM Carbonaceous Chondrites: Microtextures of a Layered Mineral Containing Fe, S, O and Ni. *Geochimica et Cosmochimica Acta* 49: 2149–63.
- Torrano, Z. A., Brennecka, G. A., Williams, C. D., Romaniello, S. J., Rai, V. K., and Wadhwa, M. 2019. Titanium Isotopic Systematics of Calcium–Aluminum-Rich Inclusions from a Variety of CV3 and CK3 Chondrites: Implications for Mixing in the Early Solar System. *Geochimica et Cosmochimica Acta* 263: 13–30.
- Trinquier, A., Elliott, T., Ulfbeck, D., Coath, C., Krot, A. N., and Bizzarro, M. 2009. Origin of Nucleosynthetic Isotope Heterogeneity in the Solar Protoplanetary Disk. *Science* 324: 374–6.
- Ushikubo, T., Jenner, T. J., Hiyagon, H., and Kita, N. T. 2017. A Long Duration of the ¹⁶O-Rich Reservoir in the Solar Nebula, as Recorded in Fine-Grained Refractory Inclusions from the Least Metamorphosed Carbonaceous Chondrites. *Geochimica et Cosmochimica Acta* 201: 103–22.
- Weiss, B. P., Bai, X.-N., and Fu, R. R. 2021. History of the Solar Nebula from Meteorite Paleomagnetism. *Science Advances* 7: eaba5967.
- Williams, C. D., Janney, P. E., Hines, R. R., and Whadwa, M. 2016. Precise Titanium Isotope Compositions of Refractory Inclusions in the Allende CV3 Chondrite by LA-MC-ICPMS. *Chemical Geology* 436: 1–10.
- Zhang, B., Chabot, N. L., and Rubin, A. E. 2022. Compositions of Carbonaceous-Type Asteroidal Cores in the Early Solar System. *Science Advances* 8: eabo5781.
- Zhang, J., Dauphas, N., Davis, A. M., and Pourmand, A. 2011. A New Method for MC-ICPMS Measurement of Titanium Isotopic Composition: Identification of Correlated Isotope Anomalies in Meteorites. *Journal of Analytical Atomic Spectrometry* 26: 2197–205.

SUPPORTING INFORMATION

Additional supporting information may be found in the online version of this article.

Material S1. Chemical compositions of CAIs and bulk WIS 91600.

Material S2. Correction of Ti isotopic compositions.

Material S3. Details on paleomagnetic remanence measurements of WIS 91600.

Material S4. Monte Carlo simulations.
